Feasibility Evaluation of Near-Field Communication in Clay with 1-mm^3 Antenna

Jin Kono, Masanori Hashimoto, Takao Onoye
Dept. Information Systems Engineering, Osaka University
Email: {kouno.jin, hasimoto}@ist.osaka-u.ac.jp

***Abstract*—We are working toward actualizing a real-time 3D modeling system that uses a sensor network consists of many 1mm^3-class sensor nodes in plastic clay. This paper focuses on 1mm^3-class small antenna and discusses the feasibility of near-field communication with such small antennas. In order to clarify communication characteristics for evaluating the feasibility, we designed 1mm^3-class spiral antennas having three different resonant frequencies and carried out 3D full-wave electromagnetic simulations. When two antennas are embedded in a clay model with 10mm distance, the maximum $|S_{21}|$ values at 30MHz, 340MHz, and 1.3GHz are -81.1dB, -69.6dB, and -64.7dB, respectively. This simulation result suggests that the near-field communication with 1mm^3-class antennas is feasible.**

***Keywords*—Small antenna, Spiral antenna, Near-field communication, 3D full-wave electromagnetic field simulation, Wireless sensor network**

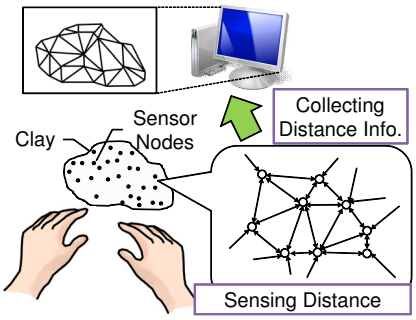

Fig. 1. "iClay" concept for real-time 3D shape acquisition.

I. Introduction

3D modeling is widely used in various fields such as video games, movie and CAD tools, and various tools and interfaces for 3D modeling have been studied for making their usage more intuitive. For this purpose, we have devised a concept called "iClay", which is illustrated in Fig. 1, and are working for its actualization [1]. In this iClay system, a number of 1mm^3-class tiny sensor nodes are distributed in plastic clay and they organize a wireless sensor network. Each sensor node senses distances to adjacent nodes and these distance information is wirelessly transmitted to a computer through the sensor network. The computer calculates relative node positions and reproduces the 3D object based on the distance information.

Recently, 1mm^3-class small antennas have been reported [2][3][4], and they are used for intra-/inter-chip communication, sensing, etc. These antennas communicate in air or through a substrate. In these communications, the antenna directions are fixed, which is different from the situation in which iClay sensor nodes are supposed to work.

This paper focuses on a small antenna for node-to-node near-field communication in iClay system. For such an antenna, there are two requirements in addition to its small volume of 1 mm^3. First, the antenna needs to have high gain to make transmitters and receivers consume less power, since the energy stored in each small sensor node is very limited. Second, in iClay, the positions and directions of sensor nodes randomly change, and hence the omni-directional antenna is desirable. We thus evaluate the gain and directionality of the antenna. On the other hand, in designing the antenna, there are unclear points; how the clay affects the communication, what is the optimum resonant frequency for iClay purpose, and how far the antenna can communicate in the clay. This paper is the first step to clarify these unclear points.

II. Antenna Design for iClay

In wireless communication, resonant frequency is a key parameter that determines the transmission rate and communication characteristics. For example, as the resonant frequency becomes higher, higher transmission rate becomes possible, which is desirable for real-time 3D modeling. However, in case of the higher resonant frequency, the design of transmitter and receiver circuits is more difficult, the circuit scale tends to be larger, and those circuits consume more power. Beside, the sensor nodes are supposed to wirelessly receive the power, and then the energy available for the communication is limited. To aid the system-level exploration of the optimal resonant frequency, this work evaluates the transmission characteristics at three frequencies.

Besides, as the antenna size becomes smaller, the resonant frequency becomes higher in general. Due to this, a small antenna is difficult to operate at low frequency. On the other hand, we want to evaluate the transmission characteristics at a wide range of frequency, and then we need to design antennas which can have various resonant frequencies while the antenna volume is kept constant. For such a purpose, a spiral inductor with parallel LC resonance is suitable and is selected in this work. Fig. 2 shows a simulation model of a small planar spiral antenna which is made of copper on an FR-4 substrate. Thanks to the parallel LC resonance, it can operate at a wide range of frequency by adjusting capacitance C_1. Capacitance C_2 is used to remove reactance. In addition, we slightly shifted the operating frequency of each antenna from its resonance

 978-1-4799-1472-2/13/$31.00

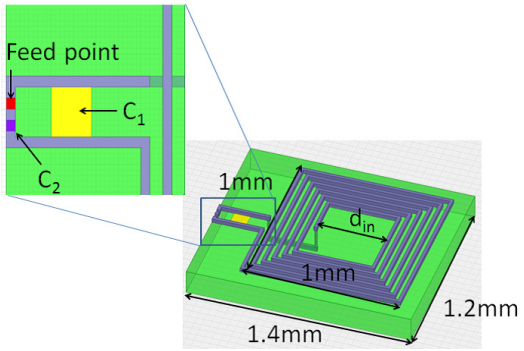

Fig. 2. Designed small spiral antenna.

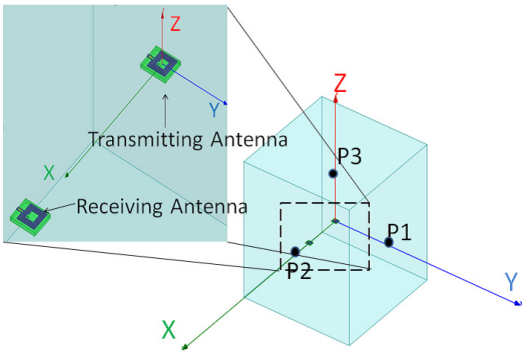

Fig. 3. Simulation Model.

TABLE I. PHYSICAL DIMENSIONS OF SPIRAL INDUCTORS USED FOR EXPERIMENTS.

Spiral inductor name	turns N	Inner diameter d_{in}[mm]
SI1	2	0.862
SI2	6	0.421
SI3	10	0.078

TABLE II. CAPACITANCE C_1 AND C_2 VALUES USED IN EXPERIMENTS.

Spiral inductor	Resonant freq. f_r	C_1	C_2
SI1	30MHz	3.0nF	1.0nF
	340MHz	22.7pF	6.8pF
	1.3GHz	1.3pF	0.32pF
SI2	30MHz	0.75nF	0.52nF
	340MHz	4.7pF	1.5pF
	1.3GHz	0.14pF	0.19pF
SI3	30MHz	0.55nF	0.17nF
	340MHz	3.5pF	1.4pF
	1.3GHz	0.045pF	0.18pF

frequency so that the input impedance of the antenna becomes 50 Ω. In this study, we selected three resonant frequencies of 30MHz, 340MHz, and 1.3GHz and simulated the antenna at these frequencies (strictly speaking, the simulated frequency is different from the resonant frequency, but the difference is very small and hereafter we do not differentiate the simulated frequency from the resonant frequency) using HFSS of ANSYS, Inc., where HFSS is a 3D full-wave electromagnetic simulator.

When using the spiral inductor with the parallel LC resonance, we can use various physical dimensions having different inductances for the same resonance frequency by adjusting the capacitance. To evaluate the impact of the physical dimensions and corresponding inductance values on the communication characteristics, we used three spiral inductors SI1, SI2 and SI3, which are different in the number of turns N and the inner diameter d_{in} as listed in Table I. Other parameters, which are the line width, the line space, the substrate thickness and the line thickness, were set to 0.02mm, 0.029mm, 0.1mm and 0.02mm, respectively, where these values were commonly used for SI1 to SI3. Table II lists C_1 and C_2 values used for the experiments. In the following, we name each antenna as a combination of the spiral inductor and resonant frequency like SI1-30MHz.

III. SIMULATION RESULTS

A. Simulation setup

To simulate electro-magnetic field in the clay, we need to consider electrical characteristics of the clay. [1] reported the measured relative permittivity and dielectric loss tangent of a resin clay up to 30 MHz. While a moderate frequency dependency is observed, this study models the clay as a lossy medium whose relative permittivity and dielectric loss tangent are 4.0 and 0.05, respectively. The measurement of these parameters at higher frequency is one of our future works.

Fig. 3 shows a simulation model to evaluate the communication characteristics, where two antennas are placed in the clay model of a 30mm × 30mm × 30mm cube. The transmitting antenna is located on the X-Y plane at the origin. In order to evaluate the influence of relative positions and directions of the antennas, the position of the receiving antenna is placed at P1 to P3 as shown in Fig.3. Those coordinates (X, Y, Z) are P1 (0mm, 10mm, 0mm), P2 (10mm, 0mm, 0mm), and P3 (0mm, 0mm, 10mm). In addition, the transmitting antenna is rotated counterclockwise along Y axis per 30°.

We evaluate forward transmission coefficient $|S_{21}|$ as a metric of communication characteristics. $|S_{21}|$ is represented as $10\log\frac{P_r}{P_{in}}$, where P_{in} is the incident power of the transmitting antenna and P_r is the received power. Besides, before evaluating the transmission characteristics, we investigated the return loss $|S_{11}|$ to confirm the impedance matching at the resonant frequencies of interest. $|S_{11}|$ values of all the antennas were less than -20dB except for SI1-30MHz. In this configuration, the input impedance of 50Ω cannot be attained.

B. Results

Fig. 4 shows $|S_{21}|$ in case that the receiving antenna is located at P1. As explained above, the transmitting antenna is rotated along Y axis, and then the angular dependency of $|S_{21}|$ is presented in Fig. 4. We can see that $|S_{21}|$ becomes the minimum at 90° and 270°. At these angles, the transmitting and receiving antennas are placed orthogonally, and there is little linkage of magnetic flux between them. On the other hand, excepting 90° and 270°, $|S_{21}|$ is roughly uniform. This tendency is found for all the antennas, while the magnitude is different. Even at different locations of P2 and P3, the tendency is similar.

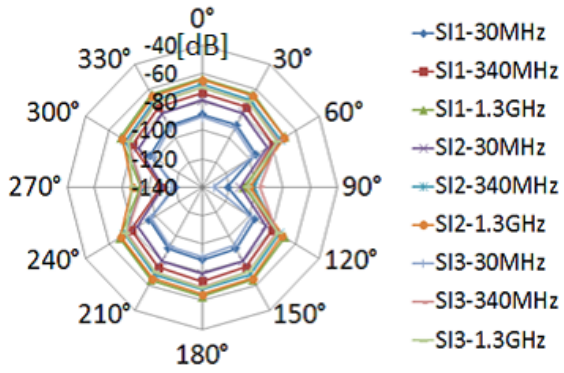

Fig. 4. Angular dependency of $|S_{21}|$ at P1.

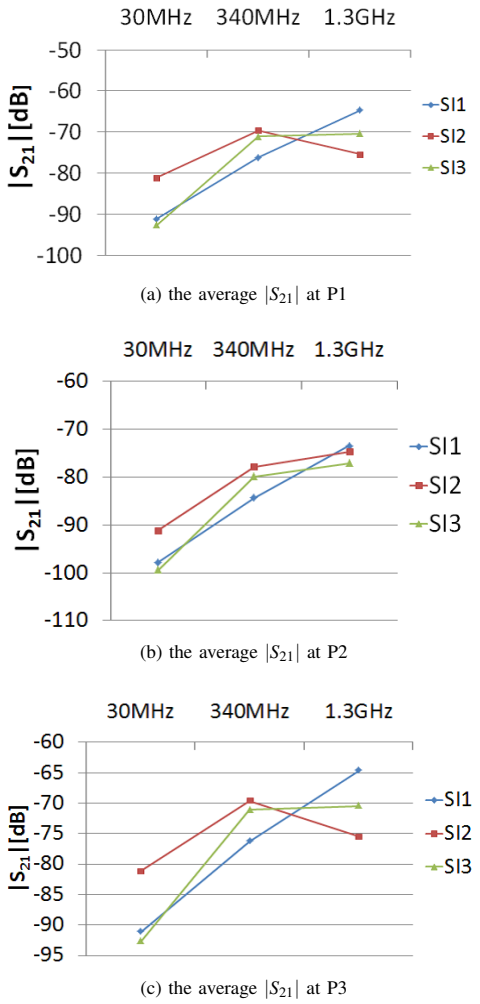

(a) the average $|S_{21}|$ at P1

(b) the average $|S_{21}|$ at P2

(c) the average $|S_{21}|$ at P3

Fig. 5. Average $|S_{21}|$ at P1, P2 and P3.

Fig. 5 shows the average values of $|S_{21}|$ at P1, P2 and P3, where we computed the average of $|S_{21}|$ over 0° to 330° angles to make it easier to distinguish the magnitude difference. At 1.3GHz, the average of $|S_{21}|$ becomes the maximum when SI1 is used. On the other hand, at 30MHz and 340MHz, SI2 attained the largest $|S_{21}|$. We suppose that this result is related to the conductor resistance of the spiral inductor and the Q-factor of the LC-parallel resonator. We will study the relation between $|S_{21}|$ and the design parameters of the spiral antenna for optimal antenna design.

Besides, the maximum values of the average $|S_{21}|$ at 30MHz, 340MHz, and 1.3GHz are -81.1dB, -69.6dB, and -64.7dB, respectively. In this evaluation, SP1-1.3GHz attained the best transmission characteristics. On the other hand, higher resonant frequency may increase power dissipation of the transmitter and receiver. Further analysis taking into account the system-level requirement is included in our future works.

We finally discuss the feasibility of the near-filed communication in the clay using the antennas described above. Reference [3] reported a 10mm-long signal transmission at 3GHz using a 4mm antenna. In this configuration, S_{21} is -70 dB, and this number is close to our results. This suggests that the near-filed communication in the clay would be possible. On the other hand, for reducing power dissipation, higher $|S_{21}|$ is strongly desirable, and we will explore more optimal antenna design for our iClay application.

IV. Conclusion

This paper evaluated the transmission characteristics ($|S_{21}|$) between 1mm^3-class small antennas in the clay, and investigated the difference of $|S_{21}|$ at three resonant frequencies. In this evaluation, a spiral antenna with two turns at 1.3GHz attained the highest $|S_{21}|$ of -64.7dB for 10mm-long communication, which suggests that the 10mm-long communication in the clay would be possible. Our future work includes investigating the optimal antenna design for iClay system taking into account both the antenna physics and system-level requirement.

References

[1] T. Shinada, M. Hashimoto, and T. Onoye, "Proximity Distance Estimation Based on Capacitive Coupling between 1mm^3 Sensor Nodes," in *Proc. International NEWCAS Conference,* 2013.

[2] B. J. Gu, W. H. Lee, K. Sawada, M. Ishida, "Wireless smart sensor with small spiral antenna on Si-substrate," *Microelectronics Journal*, vol.42, issue 9, pp.1066-1073, Sep. 2011.

[3] N. Sasaki, K. Kimoto, W. Moriyama, and T. Kikkawa, "A Single-Chip Ultra-Wideband Receiver With Silicon Integrated Antennas for Inter-Chip Wireless Interconnection," *IEEE Journal of Solid-State Circuits*, vol. 44, no.2, Feb. 2009.

[4] F. Zito, F. Aquilino, L. Fragomeni, M. Merenda, F. G. D. Corte, "CMOS wireless temperature sensor with integrated radiating element," *Sensors and Actuators*, vol.158, issue 2, pp.169–175, March 2010.